MOLECULAR AND CELLULAR BIOLOGY, Nov. 1994, p. 7394–7403
0270-7306/94/$04.00+0

Vol. 14, No. 11

Mapping an Initiation Region of DNA Replication at a Single-Copy Chromosomal Locus in *Drosophila melanogaster* Cells by Two-Dimensional Gel Methods and PCR-Mediated Nascent-Strand Analysis: Multiple Replication Origins in a Broad Zone

TOMOYUKI SHINOMIYA* AND SAWAKO INA

Mitsubishi Kasei Institute of Life Sciences, Machida, Tokyo 194, Japan

Received 22 February 1994/Returned for modification 28 April 1994/Accepted 10 August 1994

We have mapped an initiation region of DNA replication at a single-copy chromosomal locus in exponentially proliferating *Drosophila* tissue culture cells, using two-dimensional (2D) gel replicon mapping methods and PCR-mediated analysis of nascent strands. The initiation region was first localized downstream of the DNA polymerase α gene by determining direction of replication forks with the neutral/alkaline 2D gel method. Distribution of replication origins in the initiation region was further analyzed by using two types of 2D gel methods (neutral/neutral and neutral/alkaline) and PCR-mediated nascent-strand analysis. Results obtained by three independent methods were essentially consistent with each other and indicated that multiple replication origins are distributed in a broad zone of approximately 10 kb. The nucleotide sequence of an approximately 20-kb region that encompasses the initiation region was determined and searched for sequence elements potentially related to function of replication origins.

Accumulating data on chromosomal replication origins in *Saccharomyces cerevisiae* have revealed that the replication origins are defined by specific sequences and that DNA replication initiates at short DNA stretches of several hundred base pairs (see references 13, 23, and 38 for reviews). In contrast, controversial results have been reported for chromosomal replication origins in higher eukaryotes (see references 2, 12, 16, 18, and 20 for reviews).

The most extensively studied chromosomal replication origins in mammalian cells are those located downstream of the dihydrofolate reductase (DHFR) gene of Chinese hamster ovary (CHO) cells. By using a methotrexate-resistant cell line in which the DHFR gene locus had been amplified about 1,000-fold, two initiation sites were identified by mapping the earliest labeled restriction fragments at the onset of S phase in synchronized cells (18). However, analyses with recently developed replicon mapping methods have produced apparently contradictory data on the distribution of origins in the DHFR locus. Application of the two-dimensional (2D) gel electrophoretic methods developed by Brewer and Fangman (3) and Huberman et al. (24) to the amplified DHFR domain suggested that replication origins are distributed in a nearly 30-kb region including the two initiation sites identified by pulse-labeling experiments (15, 46). According to a recent report by Dijkwel and Hamlin (14), the initiation zone has been further extended to 55 kb. On the other hand, application of PCR-mediated nascent-strand analysis developed by Vassilev and Johnson (43) to exponentially growing cells containing the nonamplified, single-copy DHFR gene locus showed that DNA replication initiates at a rather fixed region coinciding with one of the early replicating sequences (45). Burhans et al. (5) further narrowed the initiation site to a fragment of 0.45 kb by mapping the site where strand specificity of the Okazaki fragments switches. Results consistent with the notion of defined localization of the replication origin were also reported by analyzing the strand specificity of leading strands in cells treated with emetine, which was shown to preferentially inhibit Okazaki fragment synthesis (6).

The 2D gel methods have also been used to examine several other chromosomal replication origins in higher eukaryotes. The existence of multiple initiation sites within a 6- to 8-kb zone was suggested for amplified chorion genes in *Drosophila melanogaster* (10, 19) and for DNA puff II/9A in *Sciara coprophila* (33), although the major initiation sites seemed to be located within the central region. The 2D gel techniques were also used to demonstrate that replication initiates at multiple sites throughout most of the 31-kb nontranscribed spacer of human ribosomal DNA (34). On the other hand, the presence of a localized replication origin was reported in the upstream region of the c-*myc* gene (44), the enhancer region of the murine immunoglobin heavy-chain gene (1, 27), and the adenosine deaminase region (47) by using the PCR-mediated nascent-strand analysis.

Thus, the 2D gel methods seem to give results supporting a broad distribution of replication origins, while direct analysis of nascent strands suggests a more fixed location of replication origins. However, our previous results for the histone gene repeats in *Drosophila* tissue culture cells indicated that both the 2D gel methods and PCR-mediated nascent-strand analysis gave essentially consistent results showing that replication initiates at multiple sites in the 5-kb histone gene repeating unit (42). In this work, we have analyzed replication origins at a single-copy chromosomal locus in exponentially growing *Drosophila* tissue culture cells, using two 2D gel methods and PCR-mediated nascent-strand analysis. The results showed, independent of the methods, that DNA replication initiates at multiple sites within a broad zone of approximately 10 kb in the initiation region identified downstream of the DNA polymerase α gene.

* Corresponding author. Mailing address: Mitsubishi Kasei Institute of Life Sciences, 11 Minami-ooya, Machida, Tokyo 194, Japan. Phone: 427-24-6251. Fax: 427-24-6317.

TABLE 1. Synthetic oligonucleotides for primers and probes

Segment	Nucleotide positions[a]				
	Primer for amplification of segments		Oligonucleotide probe	Primer for preparation of probes	
	5′	3′		5′	3′
α	4345–4364	4611–4630	4417–4437	4417–4437	4588–4607
C	1874–1893	2117–2136	1968–1988	1968–1988	2095–2114
D	5093–5112	5329–5348	5202–5222	5116–5135	5302–5321
E	7968–7989	8158–8177	8051–8071	8005–8024	8132–8151
F	10239–10258	10518–10537	10482–10502	10257–10276	10488–10507
A	12798–12817	13018–13037	12919–12939	12851–12870	12992–13011
B	15204–15223	15461–15480	15303–15323	15303–15323	15423–15442
G	17406–17425	17672–17691	17510–17530	17510–17530	17652–17671
H	20628–20647	20846–20865	20766–20786	20696–20715	20829–20848

[a] Nucleotide numbers of oligonucleotides for segment α are from Hirose et al. (22); those of oligonucleotides for the other segments are from the sequence determined in this work; nucleotide 1 is the left *Eco*RI recognition site in the region shown in Fig. 2F. Oligonucleotides shown in the second and third columns are 5′ and 3′ primers used to amplify the segments indicated in the first column. Oligonucleotides shown in the fourth column are probes for hybridization in the experiment shown in Fig. 6A. Primer sets shown in the fifth and sixth columns were used to prepare probes for hybridization in the experiment shown in Fig. 6B.

MATERIALS AND METHODS

Cells and cultivation. *D. melanogaster* Kc cells were grown at 25°C in a Spinner flask with M3(BF) medium (9) supplemented with 2% fetal calf serum.

DNA clones. Lambda clones (λDGDPA02 and λDGDPA11) covering the DNA polymerase α gene of *D. melanogaster* Oregon R and plasmid clones of their subfragments (22) were provided by F. Hirose and A. Matsukage. A genomic clone (λ clone 102) containing the downstream region of the DNA polymerase α gene was screened from a genomic library of *D. melanogaster* Oregon R provided by Y. Nishida. Subfragments were recloned to pUC18 or pBluescript II SK$^-$ plasmids.

Analysis of replication intermediates by 2D gel electrophoresis. DNA was prepared by protocol B described before (42). Exponentially growing Kc cells (5×10^8 cells per sample) were encapsulated into microbeads of low-melting-point agarose. DNA (100 to 200 μg per sample) was prepared and digested with restriction enzymes as being encapsulated in agarose beads. Replication intermediates were enriched by chromatography on a benzoyl naphthoyl DEAE-cellulose column. Caffeine eluates were concentrated by *iso*-propanol precipitation.

Neutral/neutral (N/N) 2D gel electrophoresis (3) and neutral/alkaline (N/A) 2D gel electrophoresis (24) were carried out as described before (41) except that concentrations of agarose in the N/N 2D gel electrophoresis were 0.35% in the first-dimension electrophoresis and 0.875% in the second-dimension electrophoresis.

Southern hybridization was carried out as described before (41). Hybridization images were taken by exposing membranes to erasable phosphor imaging plates (Fuji Photo Film) and analyzed with a BAS2000 Bio Image Analyzer (Fuji Photo Film). Exposure time was 4 to 24 h.

PCR-mediated nascent-strand analysis. PCR-mediated analysis of chain length of nascent DNA strands (43) was carried out as described before (42), with the following modifications. The bromodeoxyuridine (BrdU)-labeled DNA was fractionated into 15 fractions by centrifugation in alkaline sucrose gradient. The distribution of chain length of DNA fragments in each fraction was determined by agarose gel electrophoresis. Because the chain length of DNA fragments in fractions larger than 10 could not be accurately determined, it was estimated by extrapolation of the average chain length in fractions 3 to 10. PCR amplification (30 cycles) of nascent DNA was carried out by using 5-μl samples of each fraction in the presence of the indicated combinations of primer sets. The PCR products were separated by agarose gel electrophoresis and quantitated by Southern hybridization. Probes for hybridization were either ^{32}P-5′-end-labeled oligonucleotides specific to the individual segments or short fragments within the individual segments. The latter probes were prepared by PCR amplification using total chromosomal DNA of Kc cells as a template and were labeled with [^{32}P]dATP by random priming. Nucleotide positions of synthetic oligonucleotides used as primers for PCR amplification and probes are shown in Table 1.

DNA sequencing and analysis of sequence elements. DNA sequencing was done by the dideoxy method (39), using a GENESIS 2000 fluorescence automatic sequencer (DuPont). DNA fragments to be sequenced were cloned into pBluescript II SK$^-$, and their nested deletions were generated by digestion with exonuclease III and S1 nuclease (Pharmacia) for both orientations. Plasmid DNA was prepared by using the Magic MiniPreps DNA purification system (Promega). Sequencing with double-stranded DNA was done with T3 and T7 primers (Stratagene). Sequence data were assembled with the program Gel of IG-Suite (Intelligenetics).

Local helical stability, ΔG, was calculated by the method of Natale et al. (36). Sequence similarities were searched for with the program SEQ of IG-Suite or GENETYX-MAC (Software Development).

Nucleotide sequence accession number. The sequence data reported are deposited in the DDBJ, EMBL, and GenBank DNA databases under accession number D28563.

RESULTS

Mapping replication origins at a single-copy locus by 2D gel methods. Two types of 2D gel replicon mapping methods, N/N (3) and N/A (24), have been successfully applied to map chromosomal replication origins in yeast cells. However, their application to mapping chromosomal replication origins in higher eukaryotes has been limited to amplified genome or repetitive sequences because of their low sensitivity and the difficulty in preparing chromosomal DNA suitable for analysis. Our previous results (42) showed that the agarose microbead method developed by Jackson and Cook (8, 29) was very effective in preparing intact chromatin DNA suitable for 2D gel analysis and that 1 μg of total DNA prepared from exponentially growing *Drosophila* tissue culture cells was sufficient to analyze replication origins located in the histone

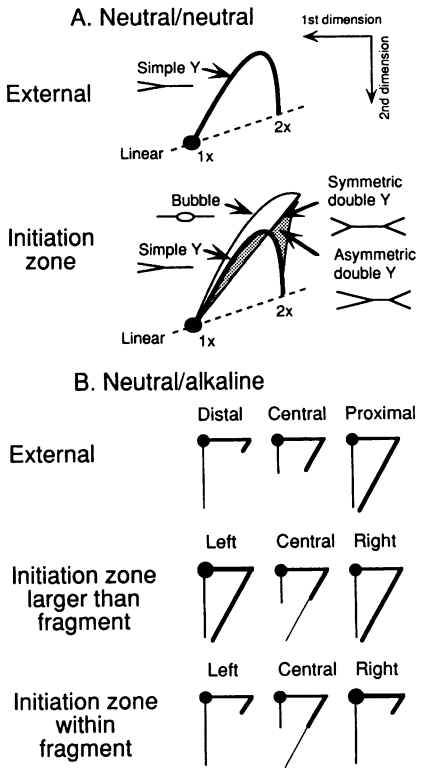

FIG. 1. 2D gel patterns expected when multiple replication origins are distributed in a large zone. The diagrams are based on those of Zhu et al. (48). In each diagram, first-dimension electrophoresis is from right to left, and second-dimension electrophoresis is from top to bottom. (A) N/N 2D gel patterns. Each panel shows the results obtained when replication origins are located outside (upper diagram) or inside (lower diagram) the studied restriction fragments. (B) N/A 2D gel patterns. Each panel shows the results obtained when the membrane containing the blot of the 2D gel is hybridized with a short probe located at the indicated position within the studied restriction fragment. When the fragment is located outside the initiation zone (top diagram), probes are at the origin-proximal end, at the origin-distal end, or in the center. When the fragment is located within the initiation zone (middle diagram) or includes the initiation zone (bottom diagram), probes are at the left end, the right end, or the center. Thick diagonal lines represent the dominant population of nascent strands, and thin diagonal lines represent faint signals from nascent strands originated from the replication origins located within the regions covered by the central probes.

repeat sequences with the N/N 2D gel method. Because copy number of the histone repeats are about 100 per haploid genome, these results suggested that it would be possible to analyze replication origins at a single-copy locus by using about 100 μg of total DNA. Actually, we could get signals derived from replication intermediates at a single-copy chromosomal locus by using 100 to 200 μg of total DNA both in N/N and N/A conditions, after one-step enrichment of replication intermediates on a benzoyl naphthoyl DEAE-cellulose column.

Diagrams shown in Fig. 1 illustrate the expected N/N and N/A 2D gel patterns when multiple replication origins are distributed in a broad initiation zone. These diagrams are based on those of Zhu et al. (48); see reference 48 for a detailed description of the differences in the 2D gel patterns between a specific origin and a broad initiation zone.

Localization of an initiation region by N/A 2D gel analysis. We first localized an initiation region in a chromosomal region including the DNA polymerase α gene by determining the direction of replication forks, using the N/A 2D gel method. A restriction map of the relevant chromosomal region is shown in Fig. 2A. Figure 2 also includes a summary of the results obtained in this work.

In the N/A 2D gel method, restriction fragments are separated mainly according to mass in the first-dimension electrophoresis, and nascent strands of replication intermediates are separated from parental strands in the second-dimension electrophoresis in alkaline conditions. By probing the blots with probes derived from different locations in the fragment, the direction of replication in the restriction fragment of interest can be determined. When the fragment is replicated by external origins, the closer a probe is to an origin, the shorter the strands it can detect, as depicted in the upper diagram of Fig. 1B.

We could locate an initiation region downstream of the DNA polymerase α gene from the data shown in Fig. 3. In fragment HH6.3, which includes the 3′ portion of the DNA polymerase α gene, the right-end probe F detected nascent strands shorter than 1 kb, while the left-end probe D detected only the largest nascent strands. The central probe E detected nascent strands greater than medium size (data not shown). These results indicate that replication proceeds unidirectionally from right to left in this fragment, opposite the direction of transcription of the DNA polymerase α gene. The direction of replication in the fragment including the 5′ portion of the DNA polymerase α gene (HH6.1) was also from right to left (data not shown). In contrast, the direction of replication in fragment EE7.0, which is located about 20 kb downstream from fragment HH6.3, was opposite that in fragment HH6.3. The left-end probe P5 of fragment EE7.0 detected nascent strands shorter than 1 kb, while the right-end probe Q1 detected only the largest nascent strands. Either of two central probes (P4 and Q2) of fragment EE7.0 detected nascent strands longer than the distance between the individual probe and the left end of fragment EE7.0 (data not shown). Thus, we could locate an initiation region somewhere between fragments HH6.3 and EE7.0. We designated this initiation region *oriDα*. The direction of replication in fragment SS9.5, which is located between fragments HH6.3 and EE7.0, seemed to be predominantly from right to left, because probe O, located close to the right end, detected nascent strands shorter than those detected by probe H, located close to the left end. Therefore, at least one replication origin seemed to be located between fragments SS9.5 and EE7.0.

N/N 2D gel analysis of the initiation region. Another type of 2D gel replicon mapping method, the N/N 2D gel method, was used to define the distribution of replication origins in *oriDα*. The N/N 2D gel method permits distinction between fragments containing internal origins (bubbles) and fragments which are passively replicated by forks moving through one end to the other (simple Y arcs) by their different electrophoretic mobilities in the second-dimension electrophoresis.

N/N 2D gel patterns of various restriction fragments located downstream of the DNA polymerase α gene are shown in Fig. 4. The N/A 2D gel data described above indicated that fragments HH6.3 and EE7.0 are replicated unidirectionally by passing forks. As expected, only simple Y arcs were visible in these fragments. In contrast to these outer fragments, composite patterns with strong simple Y arcs plus weak bubble arcs were produced by internal fragments SB6.5, EE5.7, SS6.7, and HH5.0. The bubble arcs (arrowheads in Fig. 4A) were visible up to the position of almost fully replicated molecules. The bubbles in fragment EE4.3 that overlap fragment SB6.5 were barely visible.

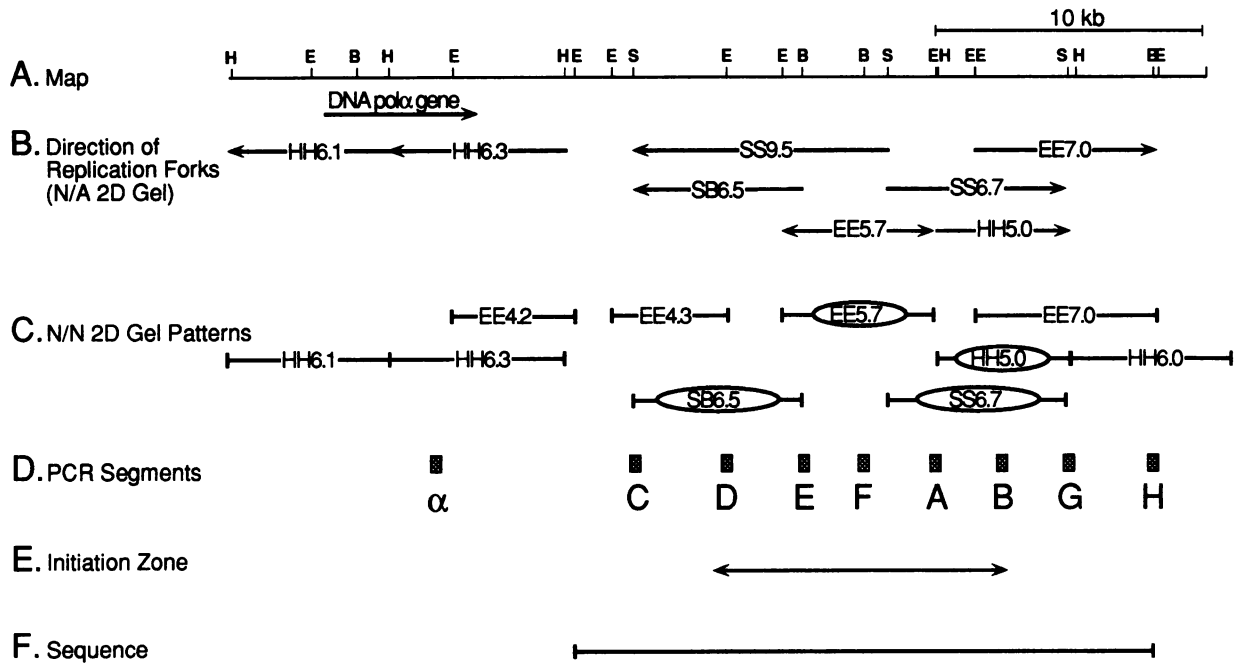

FIG. 2. Maps of the DNA polymerase α gene locus and the initiation region. (A) Physical and genetic maps. The DNA polymerase α gene and its direction of transcription are shown by an arrow under the physical map. B, *Bam*HI; E, *Eco*RI; H, *Hin*dIII; S, *Sal*I. (B) Direction of replication forks determined by N/A 2D gel analysis. The predominant direction of replication forks in each restriction fragment is shown by an arrow. A line with arrows at both ends indicates that rightward and leftward replication forks are included with nearly equal proportions. (C) N/N 2D patterns. A line with an internal bubble means that the composite arcs of simple Y arcs plus bubble arcs were observed. A simple line means that no or few bubble arcs were observed. (D) Positions of segments amplified by PCR for analysis for nascent DNA. (E) Range of the initiation region. The line with arrows at both ends represents the major initiation region of *oriD*α. (F) Range whose nucleotide sequence was determined in this work (from *Eco*RI to *Bam*HI sites).

These results confirm the location of *oriD*α suggested by the N/A 2D gel data shown in Fig. 3 and also indicate that multiple replication origins are distributed in the initiation region. Because three fragments (SB6.5, EE5.7, and HH5.0) that have no or little overlapping region generate the bubble arcs, at least three replication origins must be located in this region. Further, composite arcs with strong simple Y arcs plus weak but complete bubble arcs (schematically illustrated in the lower diagram of Fig. 1A) are indicative of distribution of multiple initiation sites in the studied restriction fragments (14, 25, 30, 35, 40–42, 46, 48). The finding that such composite arcs are observed in all restriction fragments in the initiation region suggests the presence of numerous initiation sites within *oriD*α.

We can also see signals of replication intermediates with two replication forks (double Y; lower diagram of Fig. 1A) in the 2D gel pattern produced by fragment EE5.7. Much weaker signals of the double Y's are visible also in fragments SS6.7 and HH5.0. This finding suggests that more than one initiation site within the *oriD*α are activated in the same DNA molecule at a certain frequency.

These results, including data not shown in Fig. 4, are summarized in Fig. 2C. Restriction fragments that generate composite patterns of strong simple Y arcs plus weak bubble arcs are shown by lines with internal bubbles, and those that generate no or few bubbles are indicated by straight lines. Comparison of the 2D gel patterns suggests that the majority of initiation events in *oriD*α occur within the 10-kb region shown in Fig. 2E. The distribution of initiation sites in fragment SB6.5 seems to be biased to the right portion of the fragment, because the bubbles were scarcely visible in fragment EE4.3. Similarly, the 2D gel patterns of fragments HH5.0 and EE7.0 suggest that the major initiation region does not extend into the right half of fragment HH5.0.

N/A 2D gel analysis of the initiation region. The N/N 2D gel data shown above suggest that multiple replication origins are distributed in a broad region centered at fragment EE5.7. To confirm this, three overlapping restriction fragments, SB6.5, EE5.7, and SS6.7, were subjected to N/A 2D gel analysis (Fig. 5). Each of the fragments was hybridized to four probes, two from both ends and two from the internal area of the respective fragment.

If the N/N 2D gel data are correct, fragment EE5.7 is located within the larger initiation zone. The expected N/A 2D gel patterns of a fragment that is located within an initiation zone larger than the fragment are illustrated in the middle panel of Fig. 1B. Because substantial portions of such fragments are replicated by forks moving through in both directions from external origins, both end probes will detect significant amount of short nascent strands. On the other hand, signals of short nascent strands emanating from internal replication origins located in a region covered by a central probe must be fainter than those of nascent strands originating in external origins, as illustrated with a thin line in Fig. 1B. In contrast, when the initiation region is located within the fragment, the end probes detect nascent strands longer than those detected by the central probes, as illustrated in the bottom diagram of Fig. 1B.

As shown in Fig. 5, the N/A 2D gel pattern produced by fragment EE5.7 was similar to that produced by a fragment located within a larger initiation zone. Both of the end probes detected nascent strands shorter than those detected by either of two central probes. Signals of short nascent strands emanating from internal replication origins were not detected with

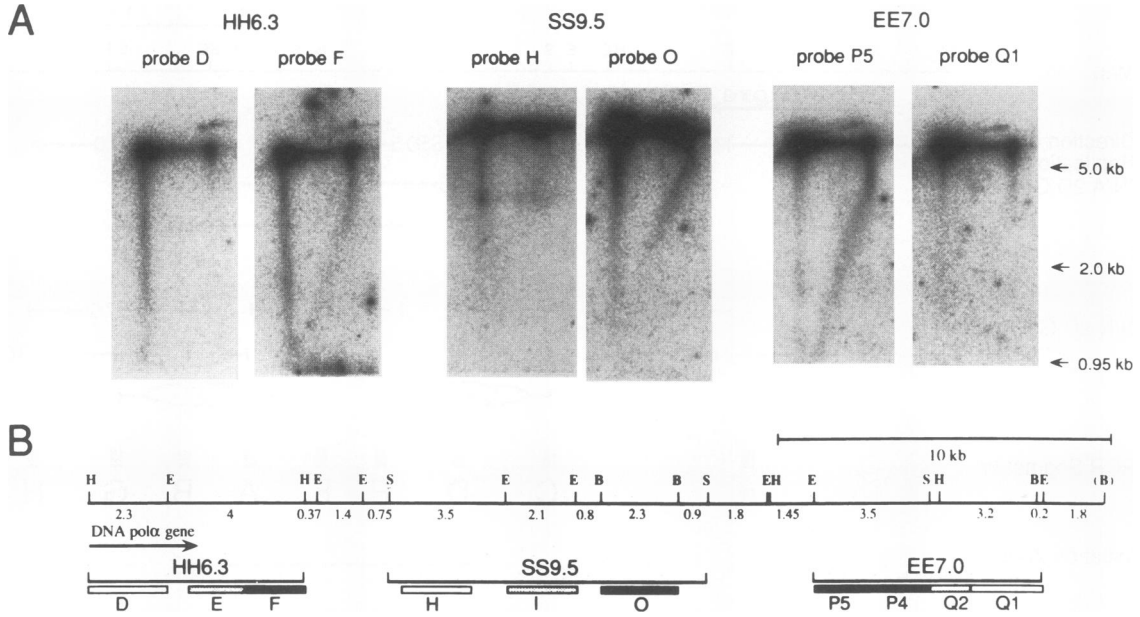

FIG. 3. Mapping of the initiation region by N/A 2D gel analysis. Restriction fragments located downstream of the DNA polymerase α gene were subjected to N/A 2D gel analysis. (A) Hybridization profiles obtained by using the left- and right-end probes of the studied restriction fragments. First-dimension electrophoresis is from right to left, and second-dimension electrophoresis is from top to bottom. (B) Locations of restriction fragments and probes. Probes shown by black boxes represent those that detected nascent DNA shorter than 1 kb; probes shown by white boxes represent those that detected only the longest nascent DNA; other probes are shaded according to the size of the shortest nascent DNA detected. Abbreviations for restriction sites are as for Fig. 2.

either of the central probes, probably because the signal-to-noise ratio in the present experimental conditions was insufficient to detect such faint signals.

In fragment SB6.5, the size of the smallest nascent strands detected by each probe increased depending on the distance of the probe from the right end of the fragment, which means that the predominant direction of replication in fragment SB6.5 is from right to left. In contrast, the predominant direction of replication forks in fragment SS6.7 was opposite that in fragment SB6.5.

These N/A 2D gel data are consistent with the N/N 2D gel data, which indicate that fragment EE5.7 is located at the center of the major initiation zone of about 10 kb.

PCR-mediated nascent strand analysis of the initiation region. The 2D gel data presented above indicate that multiple replication origins are distributed in *oriDα*. Although a similar broad distribution of replication origins was suggested by 2D gel analysis of the DHFR gene locus of CHO cells, contradictory results showing a more fixed location of the replication origin were also found with alternative replicon mapping methods. Thus, we applied the PCR-mediated nascent-strand analysis developed by Vassilev and Johnson (43) to *oriDα*.

Exponentially growing cells were pulse-labeled with BrdU, and denatured DNA was size fractionated by centrifugation in an alkaline sucrose gradient. DNA was fractionated into 15 fractions from the top of the gradient, and the BrdU-labeled nascent DNA was then purified from fractions 2 to 14. Nine segments shown in Fig. 2D were amplified by PCR using the purified nascent DNA as templates. The PCR products were separated by agarose gel electrophoresis and detected by Southern hybridization using probes specific to the individual segments.

Hybridization patterns are shown in Fig. 6. The data shown in Fig. 6A and B differ in the combinations of primer sets used for PCR amplification and in the hybridization probes used. In the experiment shown in Fig. 6A, PCR amplification was carried out with two sets of primer set combinations, B-C-D-E-F and α-A-G-H-F, and 5′-end-labeled synthetic oligonucleotides specific to the individual segments were used as probes for hybridization. Inspection of the hybridization patterns revealed that size distributions of nascent DNA are not significantly different among five internal segments, D, E, F, A, and B. In contrast to these internal segments, size distributions of nascent strands containing the outer segments are shifted to a longer size depending on the distance between the segments and the initiation region. In the experiment shown in the Fig. 6B, the same samples were amplified by the primer set combination including all of the primer sets for the internal segments (A, B, D, E, and F) and the primer set combination of the external segments (α, C, G, and H) plus segment F in order to compare the amount of nascent DNA containing the internal segments in the same amplification reaction. Further, the sensitivity of detection was increased by 10- by 30-fold by using PCR-amplified short DNA fragments labeled with random primers as hybridization probes. The results indicated that the internal segments (D, E, F, A, and B) are nearly equally found in the shortest nascent DNA, but the outer segments (α, C, G, and H) are distributed in much longer nascent DNA. (Note that hybridization intensities in some fractions larger than 8 were out of the semiquantitative range in the data shown in the Fig. 6B. Experiments using 1/10 the amount of nascent DNA were performed in parallel to provide the data for quantitative treatment described below.)

To compare quantitatively the amounts of nascent DNA, hybridization intensities of the bands were quantitated with a phosphor image analyzer, and the resulting data were used to calculate the ratios of hybridization intensity of segment F to intensities of the other segments (Fig. 7). The intensity ratio in

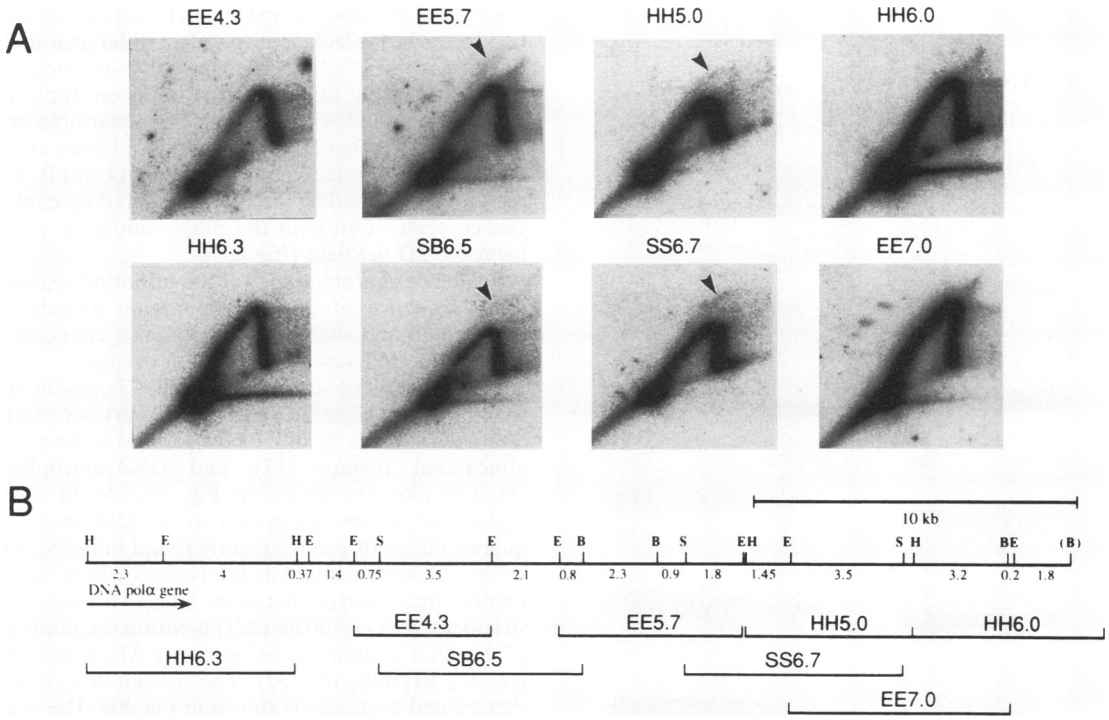

FIG. 4. N/N 2D gel patterns. Restriction fragments located downstream of the DNA polymerase α gene were subjected to N/N 2D gel analysis. (A) Hybridization profiles. First-dimension electrophoresis is from right to left, and second-dimension electrophoresis is from top to bottom. Arrowheads point bubble arcs. Probes were the restriction fragments themselves or their subfragments. (B) Locations of restriction fragments (for abbreviations, see the legend to Fig. 2).

each fraction was normalized to that in the fraction containing nascent DNA long enough to include all segments. The values estimated from the data shown in Fig. 6 were averaged and plotted versus fraction numbers. (The intensity ratios in fractions 9 to 14 [experimental conditions of Fig. 6B] were calculated from the data obtained by using 1/10 the amount of nascent DNA.) As shown in Fig. 7A and D, nascent DNA containing segment F was significantly more abundant than that containing segment α, C, G, or H until the chain length of nascent DNA reached about 30 kb or more. In contrast to these outer segments, the amount of nascent DNA containing segment D, E, A, or B was almost equal to that containing

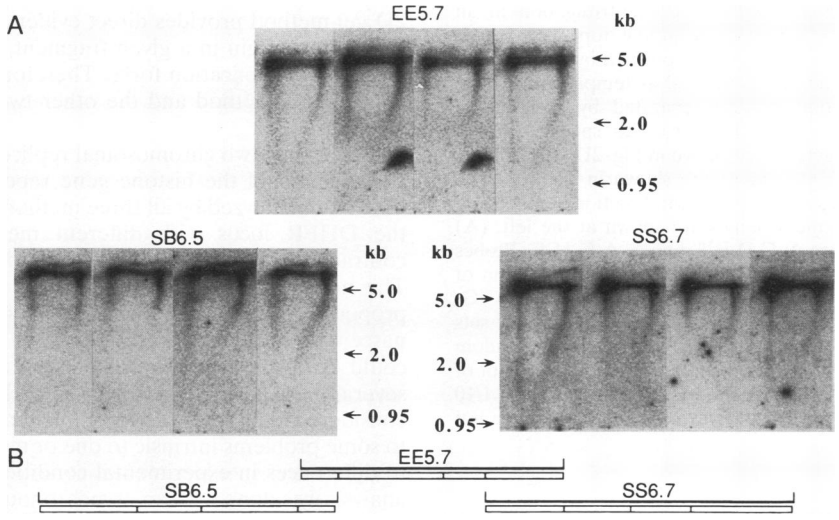

FIG. 5. N/A 2D gel patterns of the initiation region. Restriction fragments located in the initiation region defined by N/N 2D gel analysis shown in Fig. 4 were subjected to N/A 2D gel analysis. (A) Hybridization profiles. First-dimension electrophoresis is from right to left, and second-dimension electrophoresis is from top to bottom. Four panels for each restriction fragment represent, from left to right, hybridization profiles obtained by using the left-end probe, two central probes, and the right-end probe. (B) Locations of restriction fragments and probes. Probes are shown by boxes.

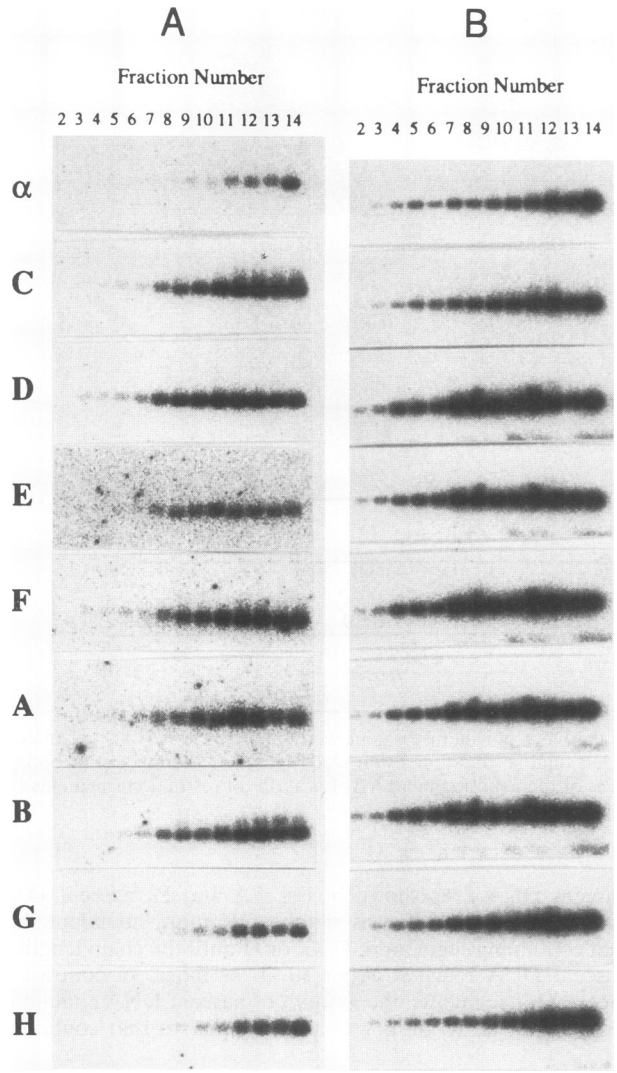

FIG. 6. Hybridization profiles of PCR-amplified nascent DNA. The BrdU-labeled DNA was fractionated by centrifugation in an alkaline sucrose gradient and collected from the top. The BrdU-labeled nascent strands in each fraction were purified by immunoprecipitation with anti-BrdU antibodies and used as templates for PCR amplification. The PCR products were separated by agarose gel electrophoresis, and the blots were hybridized to specific probes. Locations of the amplified segments are shown in Fig. 2D, and primers used to amplify the individual segments are shown in Table 1. The direction of sedimentation was from left to right. Fraction numbers are indicated at the top, and segment names are shown at the left. (A) Primer set combinations were B-C-D-E-F and α-A-G-H-F. Probes were 5′-end-labeled oligonucleotides shown in the fourth column of Table 1. (B) Primer set combinations were A-B-D-E-F and α-C-G-H-F. Probes were prepared by PCR amplification using primer sets shown in the fifth and sixth columns of Table 1 and labeled by random priming. Hybridization intensities in some larger fractions were out of the semiquantitative range in the data shown. Experiments using 1/10 the amount of nascent DNA were also performed in parallel (data not shown).

segment F (Fig. 7B and C) throughout the fractions. Similar results were obtained with two other independent DNA preparations.

These results cannot be explained by the notion that only a single specific origin is located at a short stretch of DNA within this region, because the spacing between the adjacent segments (2.3 to 2.7 kb) is sufficient to detect difference in size distribution of nascent DNA between the origin-proximal segment and the origin-distal segment in a replicon replicated from a specific origin (42, 43). Thus, the most plausible explanation of these results is that DNA replication initiates at multiple sites in a 10-kb region flanked by segments D and B. The initiation region thus defined by the PCR-mediated nascent-strand analysis coincides well with the major initiation region deduced from the 2D gel data (Fig. 2E).

Sequence characteristics of the initiation region. The nucleotide sequence of the 20.8-kb region including *oriD*α was determined and searched for sequence elements possibly related to the function of replication origins.

Distributions of sequence stretches homologous to the autonomously replicating sequence (ARS) core sequence of *S. cerevisiae* (4), the A and T boxes found in *Drosophila* scaffold attachment regions (17), and DNA-unwinding elements (DUEs) (36) are shown in Fig. 8A. As in other initiation regions of higher eukaryotes so far identified (2), these sequence elements are frequently found in *oriD*α. DUEs shown in Fig. 7A were defined as the regions where the difference in Gibb's free energy between single-stranded and double-stranded DNA of 100 bp (ΔG) is within the limits of ΔG values of the DUEs found in various yeast ARSs (less than 100 kcal [ca. 418 kJ]/mol) (36, 37). The distribution of ΔG along the determined sequence is shown in Fig. 8B. The shaded regions represent sequences where ΔG values for 100 bp are less than 100 kcal/mol.

DISCUSSION

Recently three replicon mapping methods, the N/N 2D gel method (3), the N/A 2D gel method (24), and PCR-mediated nascent-strand analysis (43), have been used to locate and characterize chromosomal replication origins in eukaryotes. The PCR-mediated method is superior in that it is sensitive enough to analyze replicons on single-copy chromosomal regions of even mammalian cells. However, the information provided by this method is essentially averaged direction of replication forks. The N/A 2D gel method also gives information on the direction of replication forks. In contrast, the N/N 2D gel method provides direct evidence for the presence of a replication origin in a given fragment, but it cannot trace the direction of replication forks. Therefore, data provided by the N/N 2D gel method and the other two methods are complementary.

So far, only two chromosomal replicons, the DHFR locus of CHO cells and the histone gene repeats in *D. melanogaster*, have been analyzed by all three methods. However, analyses of the DHFR locus with different methods gave apparently contradictory results on the distribution of replication origins. The notion of broad distribution of replication origins was proposed from 2D gel analysis (14, 46), but PCR-mediated nascent-strand analysis showed that the replication origin could be located in a much narrower region (45). Whereas several models that may solve the DHFR paradox have been considered (11), it remains possible that the discrepancy is due to some problems intrinsic to one or more of the techniques or to differences in experimental conditions. The PCR-mediated analysis was done with an asynchronous culture of a CHO cell line with a single copy of the DHFR domain (45), but most of the 2D gel data for the DHFR replicon were obtained from an extremely amplified DHFR genome and by using cells synchronized with drugs (14, 15, 46). On the other hand, our previous study using asynchronous *Drosophila* tissue culture cells (42)

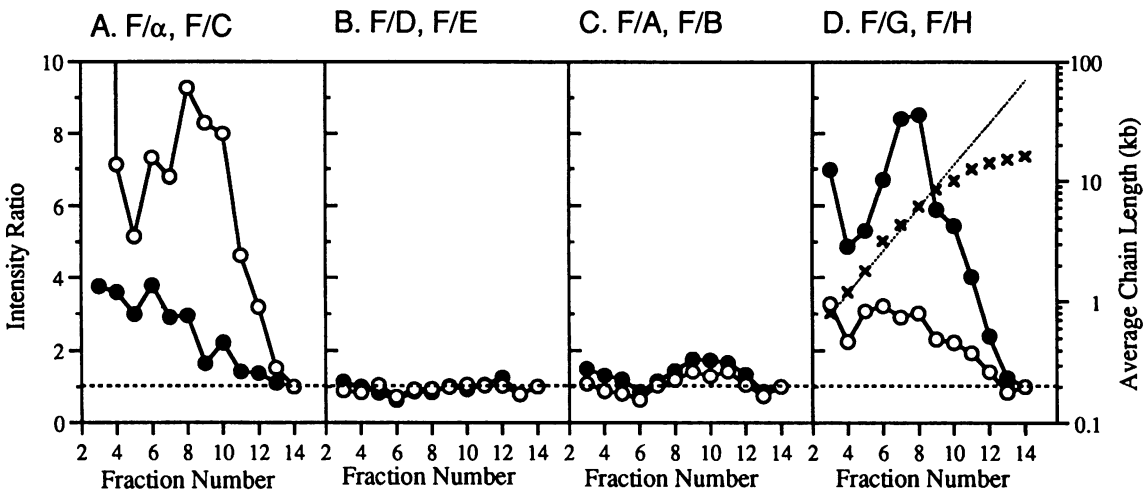

FIG. 7. Hybridization intensity ratios of PCR-amplified nascent DNA. The intensity of each hybridization band shown in Fig. 6 was measured by an image analyzer. Data for fractions 9 to 14 (experimental conditions of Fig. 6B) were based on the experiments using 1/10 the amount of nascent DNA to satisfy the semiquantitative relationship between the template DNA and hybridization intensity of the amplified products. For each fraction, intensity ratios of the segment F to intensities of the other segments were calculated. To correct for differences in amplification and hybridization efficiency, the intensity ratio in each fraction was normalized to that observed in fraction 14, in which most of the nascent DNA strands were expected to include all segments judged from their estimated size (80 kb). The values estimated from the experiments shown in the Fig. 6 were averaged and plotted versus fraction numbers. The direction of sedimentation was from left to right. (A) F/α (○) and F/C (●) ratios; (B) F/D (○) and F/E (●) ratios; (C) F/A (○) and F/B (●) ratios; (D) F/G (○) and F/H (●) ratios. ×, mean chain length of DNA fragments in each fraction; – – –, estimated chain length of DNA fragments by extrapolation of the data from fractions 3 to 10.

showed that both the 2D gel methods and the PCR-mediated method gave essentially the same result, i.e., that replication initiates at multiple sites distributed throughout the 5-kb histone gene repeating unit.

In this work, we have extended comparison of different replicon mapping methods to a single-copy chromosomal locus in asynchronous tissue culture cells of *D. melanogaster*. So far, application of the 2D gel methods to replicon analysis of higher eukaryotes has been limited to amplified or repetitive sequences. One of the technical difficulties in the 2D gel methods is how minimize the damages in replication intermediates during preparation of huge chromosomal DNA. Our

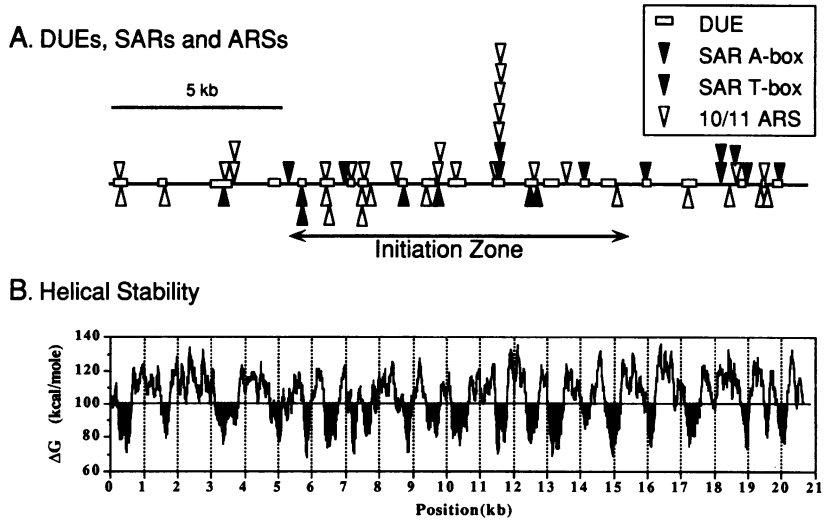

FIG. 8. Sequence elements in the initiation region. The nucleotide sequence of the 20.8-kb region including the initiation region was determined and searched for sequence elements possibly related to the function of replication origins (2). (A) Sequences homologous to the core consensus sequences of *S. cerevisiae* ARSs (10-of-11 or 11-of-11 match to WTTTATRTTTW) (4) are shown by open triangles. Sequences homologous to the A box (AATAAAYAAA) and the T box (TTWTWTTWTT) found in *Drosophila* scaffold attachment regions (SARs) (17) are shown by closed and hatched triangles, respectively. DUEs (36), shown by boxes, were defined by calculation of local helical stability represented in panel B. (B) Local helical stability (ΔG) of the initiation region and flanking region. The free energy required to strand separate a 100-bp window of DNA sequence was calculated as described by Natale et al. (36) with a 10-bp step and plotted versus the central position of the window. Regions with ΔG values below the limits of the ΔG values in the DUEs found immediately 3′ to the core consensus sequences of *S. cerevisiae* ARSs (36, 37) are shaded.

previous results (41, 42) indicated that the agarose microbead method developed by Jackson and Cook (8, 29) was very effective for preparing intact chromatin DNA with little damage in replication intermediates. The previous result (42) showed that about 1 μg of total DNA prepared by the agarose microbead method was sufficient to detect signals of replication origins in the histone gene sequences, which are repeated about 100 times. This finding suggested that replicon analysis on a single-copy chromosomal locus of *Drosophila* tissue culture cells might be possible by using about 100 μg of total DNA. Actually, as shown in the present work, we could perform 2D gel analysis of a single-copy chromosomal region by using 100 to 200 μg of total DNA after enrichment of replication intermediates. Thus, we could compare the 2D gel data with the nascent DNA analysis data in the same conditions.

The initiation region of DNA replication designated *oriD*α was first localized downstream of the DNA polymerase α gene by determining the direction of replication in various restriction fragments. The N/N 2D gel data shown in Fig. 4 indicated that the composite arcs with strong simple Y arcs plus faint but complete bubble arcs were detected for all restriction fragments covering a region of about 16 kb. These results strongly suggest that multiple replication origins are distributed within *oriD*α. The N/N 2D gel data also suggested that the primary initiation sites of *oriD*α are distributed within the 10-kb region shown in Fig. 2E. The N/A 2D gel analysis shown in Fig. 5 was consistent with these results. PCR-mediated analysis of nascent strands shown in Fig. 6 and 7 indicated that size distributions of nascent strands are not significantly different among five segments covering the 10-kb region of the primary initiation region defined by the 2D gel methods. Thus, the data obtained by 2D gel analysis and PCR-mediated nascent-strand analysis are essentially consistent with each other and indicate the presence of multiple replication origins in *oriD*α.

The present data and our previous data (42) indicate that the 2D gel methods and the PCR-mediated method are compatible and suggest that the DHFR paradox is not due to intrinsic defects in any of the methods. Our results support the notion of broad distribution of replication origins, but resolution of the DHFR paradox cannot be achieved until 2D gel data on a single-copy version of the DHFR domain are obtained by using asynchronous cells and more comprehensive analysis of nascent strands is performed over the entire region of the initiation zone defined by 2D gel analysis.

The results shown here and previous data on the histone gene repeats (42) indicate that DNA replication initiates from multiple sites in a rather broad region of 5 to 10 kb. The data can be explained by the notion that numerous potential initiation sites with relatively low sequence specificity are distributed throughout the initiation region. However, it is difficult to rule out the alternative possibility that these initiation regions are composed of several specific origin sequences. More precise mapping of initiation sites (for example, determination of strand specificity of the Okazaki fragments [5] or mapping of the 5′ ends of the Okazaki fragments) is needed to definitively distinguish among these possibilities.

Broad or random distribution of replication origins on the chromosome seems to be a general characteristic of rapidly dividing embryonic cells like *Drosophila* and *Xenopus* eggs (26, 41). Actually, in early embryos, active replication origins could be detected even in the coding region of the DNA polymerase α gene, where no replication origins were detectable in tissue culture cells (unpublished data). Thus, replication origins are confined to certain regions in tissue culture cells, unlike in embryonic cells, yet they seem to retain a dispersive nature. A series of investigations by Calos and coworkers (7, 21, 30–32) on human sequences that confer a vector plasmid to replicate autonomously in human cells seem shed some light on the nature of replication origins in higher eukaryotes. Efficiency of replication is dependent on the length of human sequences, and any human sequence longer than 20 kb has ARS activity. However, the facts that bacterial sequences of similar size are inefficient in replication activity in human cells indicates the necessity of human sequences for efficient replication in human cells. Analysis of replication intermediates by the N/N 2D gel method revealed that replication initiates at multiple sites on a plasmid containing a human sequence. A recent report showed that multiple repeats of a 3.2-kb human sequence, but not a bacterial sequence, increased the efficiency of replication dependent on the numbers of the human sequence (32). Thus, repetition of sequences abundant in the human but rare in the bacterial chromosome may be an important factor for efficient origin activity in human cells. Similar situations may also pertain to other higher eukaryotes.

One of such sequence elements may be DUEs, which are sequences in which double-stranded DNA is more easily unwound than the other regions. Such sequence elements were shown to be important for efficient replication of yeast ARSs in addition to the core consensus sequences (36, 37) and frequently found in initiation regions of higher eukaryotes (2). The importance of the DUEs in initiation of replication of yeast ARSs was also suggested by a model system using the in vitro replication system of simian virus 40 (28). Calculation of local helical stability as described by Natale et al. (36) indicated that many potential DUEs are also distributed in *oriD*α (Fig. 8). Sequences homologous to the core consensus sequence of *S. cerevisiae* ARSs and those homologous to the sequences commonly found in nuclear scaffold attachment regions are frequently found in *oriD*α as in other eukaryotic initiation regions (2). Elucidation of the roles of these sequence elements in DNA replication must await further research.

ACKNOWLEDGMENTS

We thank Fumiko Hirose and Akio Matsukage for provision of λ clones covering the DNA polymerase α gene and Yasuyoshi Nishida for provision of a genomic library of *D. melanogaster*. We also thank Fumiko Ozawa for synthesizing oligonucleotides and Yukio Ishimi for critical reading of the manuscript.

This work was partly funded by grants for scientific research from the Ministry of Education, Science and Culture, Japan.

REFERENCES

1. **Ariizumi, K., Z. Wang, and P. W. Tucker.** 1993. Immunoglobulin heavy chain enhancer is located near or in an initiation zone of chromosomal DNA replication. Proc. Natl. Acad. Sci. USA **90:** 3695–3699.
2. **Benbow, R. M., J. Zhao, and D. D. Larson.** 1992. On the nature of origins of DNA replication in eukaryotes. Bioessays **14:**661–670.
3. **Brewer, B. J., and W. L. Fangman.** 1987. The localization of replication origins on ARS plasmids in S. cerevisiae. Cell **51:**463–471.
4. **Broach, J. R., Y. Li, J. Feldman, M. Jayaram, J. Abraham, K. A. Nasmyth, and J. B. Hicks.** 1983. Localization and sequence analysis of yeast origins of DNA replication. Cold Spring Harbor Symp. Quant. Biol. **47:**1165–1173.
5. **Burhans, W. C., L. T. Vassilev, M. S. Caddle, N. H. Heintz, and M. L. DePamphilis.** 1990. Identification of an origin of bidirectional DNA replication in mammalian chromosomes. Cell **62:**955–965.
6. **Burhans, W. C., L. T. Vassilev, J. Wu, J. M. Sugo, F. S. Nallaseth, and M. L. DePamphilis.** 1991. Emetine allows identification of origins of mammalian DNA replication by imbalanced DNA synthesis, not through conservative nucleosome segregation.

EMBO J. **10**:4351–4360.
7. **Caddle, M. S., and M. P. Calos.** 1992. Analysis of the autonomous replication behavior in human cells of the dihydrofolate reductase putative chromosomal origin of replication. Nucleic Acids Res. **20**:5971–5978.
8. **Cook, P. R.** 1984. A general method for preparing intact nuclear DNA. EMBO J. **3**:1837–1842.
9. **Cross, D. P., and J. H. Sang.** 1978. Cell culture of individual *Drosophila* embryos. I. Development of wild-type cultures. Embryol. Exp. Morphol. **45**:161–172.
10. **Delidakis, C., and F. C. Kafatos.** 1989. Amplification enhancers and replication origins in the autosomal chorion gene cluster of *Drosophila*. EMBO J. **8**:891–901.
11. **DePamphilis, M. L.** 1993. Eukaryotic DNA replication: anatomy of an origin. Annu. Rev. Biochem. **62**:29–63.
12. **DePamphilis, M. L.** 1993. Origins of DNA replication in metazoan chromosomes. J. Biol. Chem. **268**:1–4.
13. **Diffley, J. F. X., and B. Stillman.** 1990. The initiation of chromosomal DNA replication in eukaryotes. Trends Genet. **6**:427–432.
14. **Dijkwel, P. A., and J. L. Hamlin.** 1992. Initiation of DNA replication in the dihydrofolate reductase locus is confined to the early S period in CHO cells synchronized with the plant amino acid mimosine. Mol. Cell. Biol. **12**:3715–3722.
15. **Dijkwel, P. A., J. P. Vaughn, and J. L. Hamlin.** 1991. Mapping of replication initiation sites in mammalian genome by two-dimensional gel analysis: stabilization and enrichment of replication intermediates by isolation on the nuclear matrix. Mol. Cell. Biol. **11**:3850–3859.
16. **Fangman, W. L., and B. Brewer.** 1992. A question of time: replication origins of eukaryotic chromosomes. Cell **71**:363–366.
17. **Gasser, S. M., and U. K. Laemmli.** 1986. Cohabitation of scaffold binding regions with upstream/enhancer elements of three developmentally regulated genes of D. melanogaster. EMBO J. **46**:521–530.
18. **Hamlin, J. L.** 1992. Mammalian origins of replication. Bioessays **14**:651–659.
19. **Heck, M. M. S., and A. C. Spradling.** 1990. Multiple replication origins are used during *Drosophila* chorion gene amplification. J. Cell Biol. **110**:903–914.
20. **Heintz, N. H., L. Dailey, P. Held, and N. Heintz.** 1992. Eukaryotic replication origins as promoters of bidirectional DNA synthesis. Trends Genet. **8**:376–381.
21. **Heinzel, S. S., P. J. Krysan, C. T. Tran, and M. P. Calos.** 1991. Autonomous DNA replication in human cells is affected by the size and the source of the DNA. Mol. Cell. Biol. **11**:2253–2272.
22. **Hirose, F., M. Yamaguchi, Y. Nishida, M. Masutani, H. Miyazawa, F. Hanaoka, and A. Matsukage.** 1991. Structure and expression during development of *Drosophila melanogaster* gene for DNA polymerase α. Nucleic Acids Res. **19**:4991–4998.
23. **Huberman, J. A.** 1992. Quest's end and questions' beginning. Curr. Biol. **2**:351–352.
24. **Huberman, J. A., L. D. Spolita, K. A. Nawotka, S. M. El-Assouli, and L. R. Davis.** 1987. The in vivo replication origins of the yeast 2μm plasmid. Cell **51**:473–481.
25. **Hyrien, O., and M. Méchali.** 1992. Plasmid replication in *Xenopus* eggs and egg extract: a 2D gel electrophoretic analysis. Nucleic Acids Res. **20**:1463–1469.
26. **Hyrien, O., and M. Méchali.** 1993. Chromosomal replication initiates and terminates at random sequences but at regular intervals in the ribosomal DNA of *Xenopus* early embryos. EMBO J. **12**:4511–4520.
27. **Iguchi-Ariga, S. M. M., N. Ogawa, and H. Ariga.** 1993. Identification of the initiation region of DNA replication in the murine immunoglobulin heavy chain gene and possible function of the octamer motif as a putative DNA replication origin in mammalian cells. Biochem. Biophys. Acta **1172**:73–81.
28. **Ishimi, Y., and K. Matsumoto.** 1993. Model system for DNA replication of a plasmid DNA containing the autonomously replicating sequence from *Saccharomyces cerevisiae*. Proc. Natl. Acad. Sci. USA **90**:5399–5403.
29. **Jackson, D. A., and P. R. Cook.** 1985. A general method for preparing chromatin containing intact DNA. EMBO J. **4**:913–918.
30. **Krysan, P. J., and M. P. Calos.** 1991. Replication initiates at multiple locations on an autonomously replicating plasmid in human cells. Mol. Cell. Biol. **11**:1454–1472.
31. **Krysan, P. J., S. B. Haase, and M. P. Calos.** 1989. Isolation of human sequences that replicate autonomously in human cells. Mol. Cell. Biol. **9**:1026–1033.
32. **Krysan, P. J., J. G. Smith, and M. P. Calos.** 1993. Autonomous replication in human cells of multimers of specific human and bacterial DNA sequences. Mol. Cell. Biol. **13**:2688–2696.
33. **Liang, C., J. D. Spitzer, H. S. Smith, and S. Gerbi.** 1993. Replication initiates at a confined region during DNA amplification in *Sciara* DNA puff II/9A. Genes Dev. **7**:1072–1084.
34. **Little, R. D., T. H. K. Platt, and C. L. Schildkraut.** 1993. Initiation and termination of DNA replication in human rRNA genes. Mol. Cell. Biol. **13**:6600–6613.
35. **Mahbubani, H. M., J. K. Elder, and J. J. Blow.** 1992. DNA replication initiates at multiple sites on plasmid DNA in *Xenopus* egg extracts. Nucleic Acids Res. **20**:1457–1462.
36. **Natale, D. A., A. E. Schubert, and D. Kowalski.** 1992. DNA helical stability accounts for mutational defects in a yeast replication origin. Proc. Natl. Acad. Sci. USA **89**:2654–2658.
37. **Natale, D. A., R. M. Umek, and D. Kowalski.** 1993. Ease of DNA unwinding is a conserved property of yeast replication origins. Nucleic Acids Res. **21**:555–560.
38. **Newlon, C. S.** 1988. Yeast chromosome replication and segregation. Microbiol. Rev. **52**:568–601.
39. **Sanger, F., S. Nicklen, and A. R. Coulson.** 1977. DNA sequencing with chain-terminating inhibitors. Proc. Natl. Acad. Sci. USA **74**:5463–5467.
40. **Schvartzman, J. B., M. L. Martínes-Robles, and P. Hernández.** 1993. The migration behavior of DNA replicative intermediates containing an internal bubbles analyzed by two-dimensional gel agarose gel electrophoresis. Nucleic Acids Res. **21**:5474–5479.
41. **Shinomiya, T., and S. Ina.** 1991. Analysis of chromosomal replicons in early embryos of *Drosophila melanogaster* by two-dimensional gel electrophoresis. Nucleic Acids Res. **19**:3935–3941.
42. **Shinomiya, T., and S. Ina.** 1993. DNA replication of histone gene repeats in *Drosophila melanogaster* tissue culture cells: multiple initiation sites and replication pause sites. Mol. Cell. Biol. **13**: 4098–4106.
43. **Vassilev, L., and E. Johnson.** 1989. Mapping initiation sites of DNA replication *in vivo* using polymerase chain amplification of nascent strand segments. Nucleic Acids Res. **17**:7693–7705.
44. **Vassilev, L., and E. M. Johnson.** 1990. An initiation zone of chromosomal DNA replication located upstream of the c-*myc* gene in proliferating HeLa cells. Mol. Cell. Biol. **10**:4899–4904.
45. **Vassilev, L. T., W. C. Burhans, and M. L. DePamphilis.** 1990. Mapping an origin of DNA replication at a single-copy locus in exponentially proliferating mammalian cells. Mol. Cell. Biol. **10**: 4685–4689.
46. **Vaughn, J. P., P. A. Dijkwel, and J. L. Hamlin.** 1990. Replication initiates in a broad zone in the amplified CHO dihydrofolate reductase domain. Cell **61**:1075–1087.
47. **Vitra-Pearlman, V. J., P. H. Gunarante, and A. C. Chinault.** 1993. Analysis of a replication initiation sequence from the adenosine deaminase region of the mouse genome. Mol. Cell. Biol. **13**:5931–5942.
48. **Zhu, J., C. Brun, H. Kurooka, M. Yanagida, and J. A. Huberman.** 1992. Identification and characterization of a complex chromosomal replication origin in *Schizosaccharomyces pombe*. Chromosoma **102**:S7–S16.